

This is a postprint version of the following published document:

Jablonski, K., Argyriou, V., Greenhill, D. y Velastin, S.A. (2015). Evaluation framework for crowd behaviour simulation and analysis based on real videos and scene reconstruction. In *6th Latin-American Conference on Networked and Electronic Media (LACNEM 2015)*.

DOI: <https://doi.org/10.1049/ic.2015.0319>

© 2015 IEEE. Personal use of this material is permitted. Permission from IEEE must be obtained for all other uses, in any current or future media, including reprinting/republishing this material for advertising or promotional purposes, creating new collective works, for resale or redistribution to servers or lists, or reuse of any copyrighted component of this work in other works.

# Evaluation Framework for Crowd Behaviour Simulation and Analysis based on Real Videos and Scene Reconstruction

Konrad Jablonski\*, Vasileios Argyriou\*, Darrel Greenhill\* and Sergio A. Velastin\*

\* Faculty of Science, Engineering and Computing Kingston University London

**Keywords:** Vision for graphics; Motion, tracking and video analysis; Cognitive and embodied vision; Crowd Simulation.

## Abstract

Crowd simulation has been regarded as an important research topic in computer graphics, computer vision, and related areas. Various approaches have been proposed to simulate real life scenarios. In this paper, a novel framework that evaluates the accuracy and the realism of crowd simulation algorithms is presented. The framework is based on the concept of recreating real video scenes in 3D environments and applying crowd and pedestrian simulation algorithms to the agents using a plug-in architecture. The real videos are compared with recorded videos of the simulated scene and novel Human Visual System (HVS) based similarity features and metrics are introduced in order to compare and evaluate simulation methods. The experiments show that the proposed framework provides efficient methods to evaluate crowd and pedestrian simulation algorithms with high accuracy and low cost.

## 1. Introduction

Crowd simulation is widely used for entertainment, education, emergency training, architectural design, urban planning, traffic engineering and numerous other applications. In most simulations a large number of agents are usually represented. The agents are expected to behave with human like actions, inside virtual surroundings avoiding obstacles and interacting with the environment or other agents. The necessity to have realistic crowd simulations has become increasingly important in such applications.

The modeling methods for crowd simulation can be separated into macroscopic and microscopic. Specifically, the movement features of the whole crowd are the main characteristic of the macroscopic algorithms [1, 2]. Microscopic methods [3, 4], operate on an individual level and are focused on including psychological and social behaviors, interaction among pedestrians, and individual decision making processes. Therefore, most of the current approaches are based on microscopic agent models providing more accurate and realistic simulation results than the macroscopic approaches.

However, one of the main problems is on estimating the accuracy of realism in a given crowd simulation. The current ways of evaluating the accuracy of crowd simulation methods are by manually extracting the ground truth and comparing it with the simulation. This approach can provide reasonable estimates, but there are significant limitations since it is a time

consuming process. Also these approaches cannot provide any indication of realism. An evaluation framework for crowd behavior simulation is proposed that correctly measures the precision of a given algorithm. This framework can determine the accuracy of any approach by introducing novel vision based features obtained from video sequences.

This paper is organized as follows: in Section 2 some related works are presented. Section 3 describes the proposed framework as well as the novel Human Visual System (HVS) based similarity features and metrics. In Section 4 the evaluation process of the proposed framework is discussed and experiments using different scenes are presented. Finally in Section 5 the conclusions are addressed.

## 2. Related Work

One of the first agent-based simulation algorithms was proposed by Reynolds in [5] focusing on birds' flocking simulation. This approach was comparable to a particle system, where agents are acting based on the environment, and they are influenced by other agents, according to a set of rules such as gravity. This paper also introduces the term *boi*, which has been used to name artificial beings from that point onwards. The  $O(n^2)$  complexity of the traversal algorithm was the major deficiency mainly due to the requirement to complete the proximity tests for each agent.

Later Helbing and Molnar [6] introduced *social forces*, which became widely successful because they could attractively emulate numerous common attributes seen in pedestrian movements and behaviors. Also, based on the principles of *social forces*, agents obtain the fundamental ability of how to navigate around other agents, obstacles, walls and various other obstructions. Over the last decades many crowd and pedestrian simulation techniques have been developed, but most of them are not concerned on the realism of simulation. Papers like [7, 8, 9, 25, 26] are primarily focusing on the performance of the algorithms, utilizing standard complexity metrics to evaluate them. By contrast, the proposed framework is focusing on estimating and evaluating the accuracy of realism in different simulations.

In order to evaluate the realism of a crowd or pedestrian simulation algorithm, vision based features and metrics are introduced in this framework. Motion estimation and tracking are few of the vision based steps applied during the process of pedestrian and crowd behavior analysis for visual surveillance in dynamic scenes. The majority of today's optical flow methods strongly resemble the original formulation of Horn

and Schunck in [10] and the one from Lucas and Kanade in [11]. The accuracy of optical flow estimation algorithms has been improving significantly over the last decade and one of the state of the art methods is the work of Sun et al in [12]. Regarding the tracking of pedestrians and crowds it is worth mentioning the methods suggested in [13] and [14]. These techniques can be used for tracking the flux of people at important public areas such as stores and travel sites, which can be automatically computed, providing congestion analysis to assist in the management of the people [15, 16].

A technique that incorporates optical flow for accuracy evaluation in crowd simulation was proposed in [17]. In this work the solution proposed to relate optical flow to physical velocity is to average the estimates of optical flow over regions of the image and then to empirically relate the average flow values to average physical velocity values by using physical velocity values determined by hand counting methods. The main issue of this approach is that it requires manual annotation and it performs well only is specific relative orientations of camera and pedestrians.

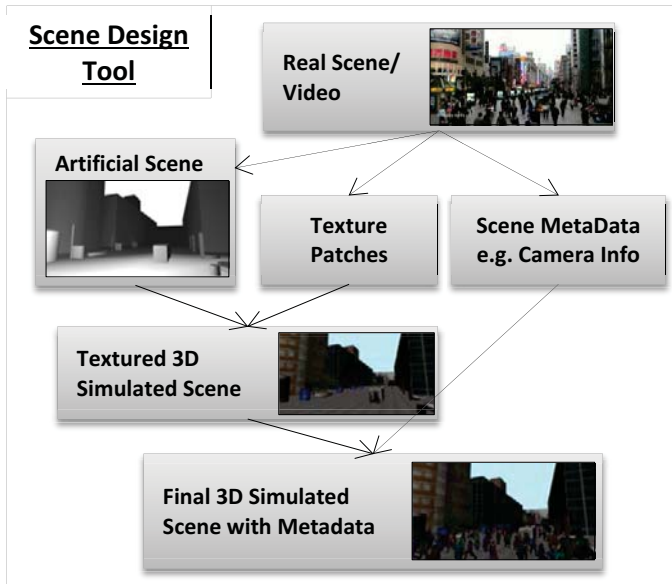


Fig. 1. Representation of the process to obtain the simulated 3D scene using the proposed scene design tool.

In other approaches, in order to evaluate the simulation accuracy, ground truth is obtained using mobile device tracking techniques [18]. In these cases obtaining the ground truth is either a time consuming process without allowing the incorporation of a large amount of scenarios or due to ethics and privacy restrictions the required data are not available. In many cases the estimation of the number of collisions occurring during the simulation process is utilized as a performance metric alongside with the required CPU or GPU processing power and time [7, 8, 27, 28]. All these approaches for pedestrian and crowd simulation evaluation either do not consider the realism parameter focusing on the performance or are applicable only to a small subset of scenes and scenarios. Furthermore, none of these methods considers Human Visual System (HVS) based similarity features and metrics, which are introduced in this work alongside the proposed novel

framework for crowd simulation evaluation based on the accuracy and the realism of the algorithms.

### 3. Proposed pedestrian and crowd evaluation Framework

The proposed framework allows the comparison of pedestrian and crowd simulation algorithms without any of the above restriction providing a novel similarity measurement. The requirements of this new framework are the availability of real footage of the observed scene or scenario using standard RGB or CCTV cameras, and an approximation of the 3D environment including the knowledge of the available exits and entrances. During the first step of the proposed novel framework, a 3D replica of the observed scene is designed using the tools provided from the framework (3D design tool). Basic primitives are utilized to build the scene such as cubes, cylinders etc., while for the texturing samples from the real video sequence are incorporated. Since the 3D scene is available the camera location and orientation are selected to be the same as in the real scene; and the entering and exiting locations are specified (see figure 1).

Regarding the simulation algorithm that is under evaluation it has been developed as a plugin in the proposed framework, obtaining the scene details and the related metadata as input parameters returning as output the simulation state in every frame. Based on this approach a new video sequence is obtained showing the simulated scene and the moving agents simulating the pedestrians' or the crowd's behavior rendered from the same point of view as in the real scene. Also, it should be mentioned that the proposed framework allows multiple algorithms for pedestrian and crowd simulation to be tested and evaluated under the same condition on the same scenarios. The system provides mechanisms to import and export scenes allowing the distribution of the evaluation scenes and the obtained results. A full description of the proposed framework is shown in figures 2 and 3 indicating all the related steps.

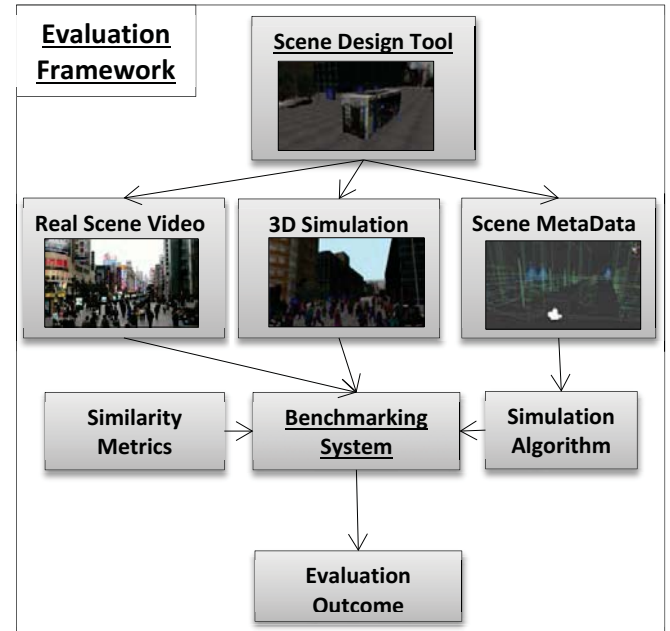


Fig. 2. Analysis of the proposed framework and the evaluation process.

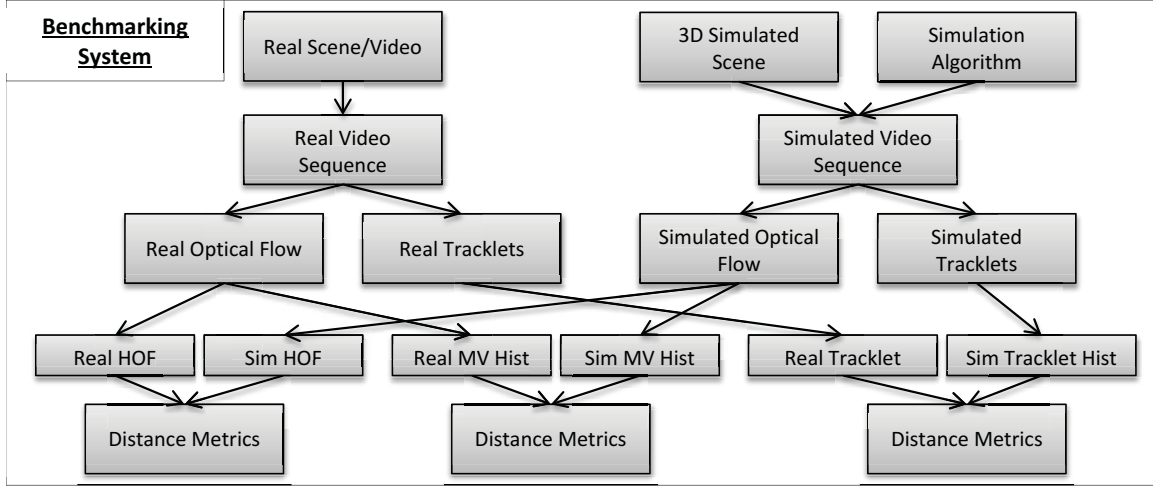


Fig. 3. Detailed analysis of the benchmarking process during the comparison of real and simulated videos

In more detail, since the 3D scene is designed using the tools provided by the proposed framework, the real and the simulated video sequences are used to extract features in order to measure their level of similarity. These features are obtained from the optical flow and the tracklets of the estimated moving objects in both sequences.

### 3.1 Optical Flow and Tracklet Estimation

An optical flow method tries to calculate the motion between two image frames which are taken at times  $t$  and  $t + \delta t$  at every pixel position [11]. Let a pixel at location  $(x, y, t)$  with intensity  $I(x, y, t)$  be moved by  $\delta x$ ,  $\delta y$  and  $\delta t$  between the two frames, the following image constraint equation can be derived

$$I(x, y, t) = I(x + ax, y + ay, t + at) \quad (1)$$

Assuming the movement to be small enough, the image constraint at  $I(x, y, t)$  can be developed with Taylor series resulting in

$$I(x + ax, y + ay, t + at) = I(x, y, t) + \frac{\partial I}{\partial x} \delta x + \frac{\partial I}{\partial y} \delta y + \frac{\partial I}{\partial t} \delta t \quad (2)$$

The equation below is derived

$$I_x V_x + I_y V_y = -I_t \quad (3)$$

where  $V_x$ ,  $V_y$ , are the  $x$  and  $y$  components of the velocity or optical flow of  $I(x, y, t)$  and  $I_x$ ,  $I_y$  and  $I_t$  are the derivatives of the image at  $(x, y, t)$  in the corresponding directions. The solution as given by Lucas and Kanade is a non-iterative method, which assumes a locally constant flow. Assuming that the flow  $(V_x, V_y)$  is constant in a small window of size  $m \times m$  with  $m > 1$ , centred at pixel  $x, y$  and numbering the pixels as  $1 \dots n$ , a set of equations is obtained

$$\begin{bmatrix} I_{x1} & I_{y1} \\ \vdots & \vdots \\ I_{xn} & I_{yn} \end{bmatrix} \begin{bmatrix} V_x \\ V_y \end{bmatrix} = \begin{bmatrix} -I_{t1} \\ \vdots \\ -I_{tn} \end{bmatrix} \Rightarrow A \vec{M} = -b \Rightarrow \vec{M} = (A^T A)^{-1} A^T (-b) \quad (4)$$

This means that the optical flow can be found by calculating the derivatives of the image in all three dimensions. A weighting function  $W(i, j)$ , with  $i, j \in [1, \dots, m]$  could be added

to give more prominence to the centre pixel of the window. Gaussian functions are preferred for this purpose, but other functions or weighting schemes are also possible. Besides, for computing local translations, the flow model can be extended to affine image deformations. Black and Anandan in [12], describe how the single motion assumption, as well as the constant brightness constraint are not always valid. They discuss how these assumptions can be relaxed in order to develop a more robust estimation framework.

Regarding the tracklet estimation many algorithms are available in the literature based on motion or other features and using particle and Kalman filters [13, 14, 19, 24]. Specifically, the problem of motion-based object tracking is divided into the part of detecting the moving objects in each frame and then associating the detections corresponding to the same object over time. Gaussian mixture models are used to apply background subtraction and the noise is eliminated using morphological operations on the obtained foreground mask.

In case of Kalman filters, the track's location in each frame is predicted and the likelihood of each detection assigned to each track is determined. The Kalman filter is a recursive estimator and this means that only the estimated state from the previous time step and the current measurement are needed to compute the estimate for the current state. The Kalman filter has two distinctive features. One is that its mathematical model is described in terms of state-space concepts. Another is that the solution is computed recursively. Usually, the Kalman filter is described by a system state model and a measurement model. The state-space model is described as a system state model and measurement model as shown in (5) and (6) respectively.

$$s(t) = O(t-1)s(t-1) + w(t) \quad (5)$$

$$z(t) = H(t)s(t) + v(t) \quad (6)$$

where  $O(t-1)$  and  $H(t)$  are the state transition matrix and measurement matrix respectively. The  $w(t)$  and  $v(t)$  are white Gaussian noise with zero mean.

Kalman filters have two phases: prediction step and correction step. The prediction step is responsible for



projecting forward the current state, obtaining a prior estimate of the state  $S(t)$ . The task of the correction step is for the feedback. It incorporates an actual measurement into the prior estimate to obtain an improved posterior estimate  $S^+(t)$ , which is written as shown in (7).

$$S^+(t) = S^-(t) + k(t)[z(t) - H(t)S^-(t)] \quad (7)$$

where  $k(t)$  is the weighting and is described as shown in (8)

$$k(t) = p^-(t)H(t)^T[H(t)p^-(t)H(t)^T + R(t)]^{-1} \quad (8)$$

In (8)  $p^-(t)$  is priori estimate error covariance. It is defined as shown in (9).

$$p^-(t) = E[e^-(t)e^-(t)^T] \quad (9)$$

where  $e^-(t) = s(t) - s^-(t)$  is the prior estimate error. In addition, the posteriori estimate error covariance is defined as shown in (10).

$$p^+(t) = E[e^+(t)e^+(t)^T] \quad (10)$$

where  $e^+(t) = s(t) - s^+(t)$  is the posteriori estimate error. The prediction step and correction step are executed recursively in the definitions as shown in (11), (12), (13), (14) and (15).

Prediction step:

$$s^-(t) = O(t-1)s^+(t-1) \quad (11)$$

$$p^-(t) = O(t-1)p^+(t-1)O(t-1)^T + Q(t-1) \quad (12)$$

Correction step:

$$k(t) = p^-(t)H(t)^T[H(t)p^-(t)H(t)^T + R(t)]^{-1} \quad (13)$$

$$s^+(t) = s^-(t)k(t)[z(t) - H(t)s^-(t)] \quad (14)$$

$$p^+(t) = [1 - k(t)H(t)]p^-(t) \quad (15)$$

The prediction-correction cycle is repeated. Looking at (13), the measurement error  $R(t)$  and Kalman gain  $k(t)$  are in inverse ratio. The smaller the  $R(t)$ , the greater the weight for the gain  $k(t)$ . In this case, the measurement is more trusted, while the predicted result is less trusted. However, as the a priori estimate error  $p^-(t)$  approaches zero, the gain  $k(t)$  weights the residual less heavily. The actual measurement is trusted less and less, while the predicted result is trusted more and more.

Optical flow and tracklet estimation is an important aspect of this framework. In this system the optical flow algorithm proposed in [12] and the tracking method presented in [19] were utilized but the system is designed in such a way that allows the incorporation of multiple motion estimation or tracking methods as plugins. Based on this system architecture the proposed evaluation framework is dynamic and capable of utilizing current and future state of the art tracking methods.

### 3.2 Similarity Metric based on Motion and Tracklet Flux

In order to evaluate the similarity level of the simulated and real scenes a new metric is required that will allow an objective comparison incorporating Human Visual System (HVS) based similarity features and metrics. According to Weber's Law [20] and the work in [21, 22] motion perception is in accordance with Weber's Law when the signal-to-noise ratio is regarded as stimulus intensity. Therefore, the minimum motion contrast  $dV$

as a function of background motion  $V$ , required for the human visual system to notice a change is expressed as

$$dm = k \frac{dV}{V} \quad (16)$$

where  $dm$  is the differential change in motion perception,  $dV$  is the differential increase in the velocity, and  $V$  is the velocity. The parameter  $k$  is to be estimated using experimental data. The proposed measure includes Fechner's Law, which relates velocity  $V$ , to perceived motion,  $m$ , as seen by the human visual system, as follows:

$$m = k \ln\left(\frac{V}{V_{max}}\right) \quad (17)$$

where  $V_{max}$  is the 'upper threshold' of the human eye. The proposed metric is based on the motion and tracklet flux histograms obtained from the perceived motion  $m$  utilizing standard computer vision algorithms.

Let us assume that  $I_R(u, t)$  and  $I_S(u, t)$  are the image frames of a real and the correspondent simulated scene, respectively. The motion vectors for each pixel location in each frame are estimated using the above optical flow techniques, which are shown in (18) and (19)

$$M_R(\mathbf{u}, t) = \mathcal{F}(I_R(\mathbf{u}, t), I_R(\mathbf{u}, t-1)) \quad (18)$$

$$M_S(\mathbf{u}, t) = \mathcal{F}(I_S(\mathbf{u}, t), I_S(\mathbf{u}, t-1)) \quad (19)$$

The estimated tracklets are obtained using motion information and Kalman filters.

$$T_R(n_R, \mathbf{u}, t) = \mathcal{F}(M_R, I_R) \quad (20)$$

$$T_S(n_S, \mathbf{u}, t) = \mathcal{F}(M_S, I_S) \quad (21)$$

Since the motion vectors and the tracklets are available the histogram of oriented optical flow (HOOOF) is calculated both for the real and simulated scenes.

$$f_R^{HOOF} = HOOF(M_R) \quad (22)$$

$$f_S^{HOOF} = HOOF(M_S) \quad (23)$$

Also, a 2D histogram of the motion parameters is obtained using (24) and (25).

$$f_R^{H2D}(r_{ij}) = m_{ij}(M_R) \quad (24)$$

$$f_S^{H2D}(r_{ij}) = m_{ij}(M_S) \quad (25)$$

Where  $r_{ij}$  is the  $i^{\text{th}}$  and  $j^{\text{th}}$  motion level in an interval  $[-G, +G]$  and  $m_{ij}$  is the number of pixels in all the given frames whose motion level is  $r_{ij}$ .

Regarding the tracklets, the time parameter in (20) and (21) is removed by superimposing all of them at the same time instance. This is performed since the similarity metric is applied on a given time interval, that can be the whole sequence or a small time fragment. In the same way as in (24) and (25) we obtain:

$$f_R^T(r_{ij}) = m_{ij}(T_R) \quad (26)$$

$$f_S^T(r_{ij}) = m_{ij}(T_S) \quad (27)$$

Finally, the flux of the features in (22-27) is represented by the surface integral of the given vector field.

$$\Phi(\mathbf{u}, t) = \sum_u \sum_t f \, dudt \quad (28)$$

Based on (28), we obtain  $\Phi_R^{HOOF}$ ,  $\Phi_S^{HOOF}$ ,  $\Phi_R^{H2D}$ ,  $\Phi_S^{H2D}$ ,  $\Phi_R^T$  and  $\Phi_S^T$  that correspond to the proposed metrics. In order to measure the similarity and rank the algorithms a set of different distances can be utilized e.g. Correlation, Bhattacharyya, Chi Square, Histogram Intersection, Dot Product, L1, Euclidean or earth mover's distance (EMD). All these metrics can be applied either on the whole sequence or on smaller blocks allowing spatiotemporal adaptation of the proposed features and metrics.

#### 4. Experiments and Results

In order to evaluate the proposed framework experiments were performed using two real scenes (see figure 4). Using the design tool, replicas of the scenes were developed utilizing basic primitives and textures from the original real frames. During the design process of the simulated 3D scenes metadata information regarding the relative camera location and orientation, the weather condition and the approximate time are manually specified. Also, all possible entrances and exits in these scenes are selected and alongside with all the metadata and the 3D scene will be provided to the simulation algorithm to populate the scene with pedestrians.



Fig. 4. Real scenes that were utilized. one outdoors and one indoors.



Fig. 5. The simulated scenes that correspond to the real ones designed using the proposed tool.

TABLE I. SPEARMAN'S RANK CORRELATION COEFFICIENT FOR BOTH SCENES USING BHATTACHARYYA DISTANCE FOR RANKING

$\rho$	Scene A	Scene B
$\Phi^{HOOF}$	0.776223776	0.468531469
$\Phi^{H2D}$	0.216783217	0.279720280
$\Phi^T$	0.174825175	0.321678322

Regarding the simulation algorithm an approach based on [23] was considered and two parameters were selected to be adjustable in our experiments, the number of pedestrians and their average speed. Frame examples of the simulated sequences are shown in figure 5 and the length and the size of each sequence were equal to the corresponding real video. In our experiments three different levels of population and four levels of speed were considered, allowing an accurate evaluation of the proposed framework and the related novel metrics. The optical flow and the tracklets were estimated (see figures 6-7) for each scene and each case of the simulated case, resulting to 24 combinations in total. Thus, the HOOF features and the 2D histograms of  $64 \times 64$  bins were calculated using the optical flow and equivalently the histograms of the tracklets

based on the equations (22-28). Examples of the obtained features are shown in figure 8 indicating that they are appropriate for Human Visual System (HVS) based similarity features.

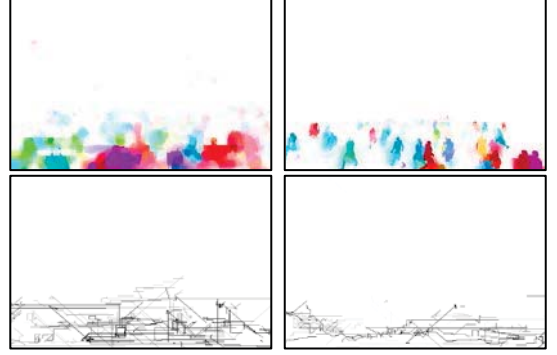


Fig. 6. Examples color coded representations of the optical flow and the tracklets for the first real (left column) and simulated (right column) scene.

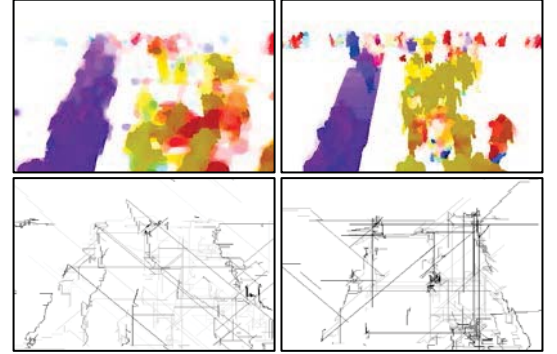


Fig. 7. Examples color coded representations of the optical flow and the tracklets for the second real (left column) and simulated (right column) scene.

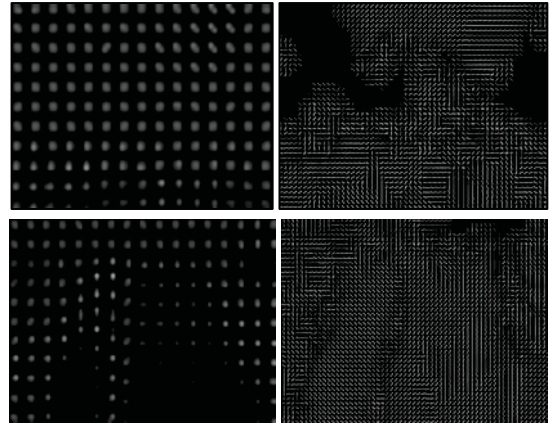


Fig. 8. The obtained features (left) local 2D histograms (right) HOOF.

In order to evaluate the performance of the suggested metrics and features in terms of similarity based on HVS, subjective experiments were performed. The mean opinion score (MOS) was utilized to further evaluate the proposed metrics. For these experiments 10 humans were asked to observe all the simulated videos side by side with the original one and provide a similarity mark between 0 and 5 with higher values indicating higher similarity. Spearman's rank correlation coefficient  $\rho$  was used to obtain the similarity between the ranked scenes for each metric. The ranking in the case of the proposed metrics was based on Bhattacharyya distance. All the results are summarized in Figure 9 and Table I indicating that

the proposed metrics and features are close to the HVS and especially the HOOF features. Also, from the results it can be observed the humans are more sensitive in motion differences than in the population size. This is shown in Tables II and III by calculating the standard deviation over each level of speed and population. It can be observed that the deviation is higher when the population is constant and the level of speed varies.

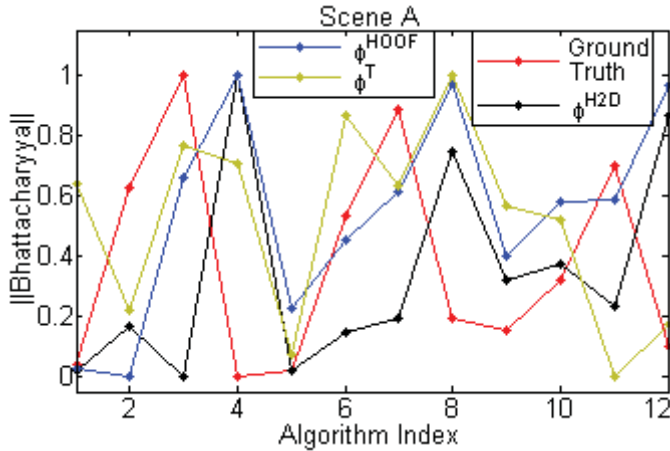


Fig. 9. Bhattacharyya distance for all the combinations of speed and population.

TABLE II. STANDARD DEVIATION OF MOS AND HOOF FOR SCENE A

Population	Speed Level				$\sigma$
	1	3	5	8	
150	0.4000	0.8000	0.5500	0.4375	<u>0.1803</u>
200	0.4625	0.925	0.6875	0.3500	<u>0.2546</u>
250	0.3375	1.0000	0.7500	0.3625	<u>0.3199</u>
$\sigma$	<u>0.0625</u>	<u>0.1010</u>	<u>0.1023</u>	<u>0.0473</u>	

TABLE III. STANDARD DEVIATION OF MOS AND HOOF FOR SCENE B

Population	Speed Level				$\sigma$
	1	3	5	8	
150	0.2500	0.8875	0.5875	0.3625	<u>0.2812</u>
200	0.3750	0.9625	0.7000	0.2875	<u>0.3099</u>
250	0.4125	1.000	0.6250	0.2875	<u>0.3119</u>
$\sigma$	<u>0.0851</u>	<u>0.0572</u>	<u>0.0572</u>	<u>0.0433</u>	

## 5. Conclusions

In this paper a novel framework for evaluation of pedestrian and crowd simulation algorithm was proposed focusing on the realism in the behavior of the agents. The suggested evaluation approach is based on the idea of recreating real video scenes in 3D environments and utilizing novel Human Visual System (HVS) based similarity features and metrics to estimate the correlation between the real and the simulated videos in terms of realism. Experiments were performed in real scenes showing that the proposed features and mainly the HVS-HOOF are well correlated with the MOS.

## REFERENCES

- [1] A. Treuille, S. Cooper, and Z. Popović, "Continuum crowds," in Proceedings of ACM SIGGRAPH, pp. 1160–1168, 2006
- [2] R. Hughes, "A continuum theory for the flow of pedestrians," Transportation Research Part B, vol.36, no.6, pp.507–535, 2002.
- [3] Q. H. Nguyen, F. D. McKenzie, and M. D. Petty, "Crowd behavior cognitive model architecture design," in Proceedings of the BRIMS, pp. 55–64, 2005
- [4] N. Pelechano, K. O'Brien, B. Silverman, and N. Badler, "Crowd simulation incorporating agent psychological models, roles and communication," in the Workshop on Crowd Simulation, 2005.
- [5] Reynolds, C. W. Flocks, Herds, and Schools: A Distributed Behavioral Model, in Computer Graphics, 21(4) SIGGRAPH pp 25-34, 1987
- [6] Kessel, A., H. Klupfel, J. Wahle, and M. Schreckenberg. Microscopic simulation of pedestrian crowd motion, in Pedestrian and Evacuation Dynamics, pp. 193-202, 2000
- [7] Ricks, B.; Egbert, P. "A Whole Surface Approach to Crowd Simulation on Arbitrary Topologies," Visualization and Computer Graphics, IEEE Trans, vol.PP,no.99,pp.1,1, 2013
- [8] Qin Gu, Zhigang Deng, "Generating Freestyle Group Formations in Agent-Based Crowd Simulations," IEEE Computer Graphics & Applications, vol.33, no.1, pp.20-31, 2013
- [9] Joselli, M.; Passos, E.B.; Zamith, M.; Clua, E.; Montenegro, A.; Feijó, B., "A Neighborhood Grid Data Structure for Massive 3D Crowd Simulation on GPU," Games and Digital Entertainment (SBGAMES), VIII Brazilian Symposium on , vol., no., pp.121,131, 8-10 Oct. 2009
- [10] Horn, B.K.P., and Schunck, B.G., Determining Optical Flow, AI(17), No. 1-3, pp. 185-203, August 1981
- [11] Lucas B. D. and T. Kanade, "An interactive image registration technique with an application to stereo vision", Proceedings of the DARPA image understanding workshop, pp.121-130, 1981.
- [12] Sun, D., Roth, S., and Black, M. J., Secrets of optical flow estimation and their principles, IEEE, CVPR, June 2010
- [13] Munder, S.; Schnorr, C.; Gavrilu, D., "Pedestrian Detection and Tracking Using a Mixture of View-Based Shape-Texture Models," IEEE Tran Intelligent Transportation Systems, v.9, n.2, pp.333,343, 2008
- [14] Michalis Raptis and Stefano Soatto, Tracklet Descriptors for Action Modeling and Video Analysis In Proceedings of the European Conference on Computer Vision, September 2010
- [15] P. Allain, N. Courty, and T. Corpetti, Crowd Flow Characterization with Optimal Control Theory, ACCV 2009
- [16] Weiming Hu; Tieniu Tan; Liang Wang; Maybank, S., "A survey on visual surveillance of object motion and behaviors," Systems, Man, and Cybernetics, Part C: Applications and Reviews, IEEE Transactions on , vol.34, no.3, pp.334,352, Aug. 2004
- [17] Clarke, T.L., D.J. Kaup, Linda Malone, Rex Oleson, Mario Rosa, 2007, Crowd Model Verification Using Video Data, EMSS 2007.
- [18] Qiang Wang; Yan Liu; Juan Chen, "Accurate indoor tracking using a mobile phone and non-overlapping camera sensor networks," IEEE International I2MTC, pp.2022,2027, 2012
- [19] W.L. Khong, W.Y. Kow, H.T. Tan, H.P. Yoong, K.T.K Kalman Filtering Based Object Tracking in Surveillance Video System. Teo 3rd CUTSE International Conference (CUTSE) 2011
- [20] Weber, E.H. De subtilitate tactus, De pulsu, resorptione, auditu et tactu: Annotationes anatomicae et physiologicae pp.44-174, 1834
- [21] Wharton, E.; Panetta, K.; Agaian, S., "Human visual system based similarity metrics," SMC. IEEE International Conference on Systems, Man and Cybernetics, vol., no., pp.685,690, 2008
- [22] Zanker, J. M. Does motion perception follow Weber's law? Perception, 24, 363-372, 1995
- [23] Wenxi Liu, Rynson Lau, Dinesh Manoch Crowd Simulation using Discrete Choice Model, IEEE VRW, v.3 no.6, pp.4-8 2012
- [24] Min Hu; Weiming Hu; Tieniu Tan, "Tracking people through occlusions," Pattern Recognition, 2004. ICPR 2004. vol.2, no., pp.724,727 Vol.2, 2004
- [25] Helbing, D., I. J. Farkas, P. Molnar, and T. Vicsek. Simulation of pedestrian crowds in normal and evacuation situations, in Pedestrian and Evacuation Dynamics, pp. 21-58, Springer- 2002
- [26] Helbing, D. 1992. A fluid-dynamic model for the movement of pedestrians, Complex Systems, 6, pp. 391-415, 1992
- [27] Kaup, D. J., J. E. Fauth, L.J. Walters, L. Malone, T. Clarke. 2006. Simulations as a mathematical tool, SIAM Conference on the Life Sciences, Raleigh, NC, Aug. 3, 2006.
- [28] Lakoba, T. I., D.J. Kaup, and N.M. Finkelstein. 2005. Modifications of the Helbing-Molnar-Farkas-Vicsek social-force model for pedestrian evolution, SIMULATION: Transactions SMSI, 81, pp 339-349, 2005.